International Journal of Industrial Engineering and Management (IJIEM), Vol. 5 No 2, 2014, pp. 53-60
Available online at www.iim.ftn.uns.ac.rs/ijiem_journal.php
ISSN 2217-2661

UDK: 621.01

Mechanism and Effect of Mallet Tapping on Contact Stress Distribution Between V-band Clamp and Piping Systems

Zhengui Zhang
Ph.D. student of Mechanical Engineering Technology, Purdue University, 401 North Grant Street, 47907, IN, USA, zhang658@purdue.edu

Haiyan H Zhang
Faculty of Mechanical Engineering Technology, Purdue University, 401 North Grant Street, 47907, IN, USA, hhzhang@purdue.edu

Peixuan Wu
Research Scientist of Mechanical Engineering Technology, Purdue University, 401 North Grant Street, 47907, IN, USA, peixuan@purdue.edu

Received (02.02.2014.); Revised (27.05.2014.); Accepted (30.06.2014.)

Abstract

This paper is dedicated to investigate the mechanism of mallet tapping on the equalization of contact pressure distribution between V-band clamp and piping system. A sensor platform with charge mode amplifier is built to collect quasi-static measurements of contact pressure during loading. Contact pressures in the initial stage before and after mallet tapping is measured using piezoelectric sensor tests. Finite element analysis (FEA) is carried out to find the initial contact areas. The controlled measurement verified the viability of mallet tapping on contact pressure redistribution. In terms of clamping stability, the effect of mallet tapping is discussed from the working principle of Vibratory Stress Relief (VSR). Dynamic analysis is also tried to explore the mechanism of mallet tapping on equalizing the contact pressure distribution. The frequencies of clamp are estimated by theoretical calculation and experiment tests, which are applied to derive the mode of vibration wave after mallet tapping.

Key words: *Contact pressure, Mallet tapping, V-band clamp, VSR*

1. INTRODUCTION

Tubing closures connection, such as exhaust piping systems, with V-band clamps are a proven and economical way for decades in high temperature, high pressure or vibration conditions. V-band clamps fasten with only one T-bolt are inexpensive and convenient in assembly and maintenance, especially when install and uninstall are frequently required. At the same time, as the operation conditions become more and more challenge, reliable and persistent clamp connection are extremely important and highly valued in industries, especially in the aerospace industry where clamps are applied in exhaust systems, filters, pumps and so on. However, the knowledge of the clamp assembly and condition of service was not well documented and publicized. Even worse, most the reachable publications are not well investigated or remain empirical approached. Thus, V-band clamp theoretical and the relevant research in this uninformed environment turn to be more demanding[1]. V band clamp is composed on two parts, V band and V-retainers. Torque applied on the T-bolt nut generates circumferential tension and overcome friction between V-retainers and piping system when two ends of clamp are drew to each other. The circumferential tension is transmitted to an inward radial force and then created an axial load to seal the components of piping systems with the wedging action from the V-retainer[2, 3]. Friction helps to prevent relative slipping or loose connection between clamp and piping systems during service. However, the existence of friction also leads to exponential distribution of contact pressure which is not pleasing in V-band clamp connection [2]. A tight and uniform contact pressure between clamp and piping systems are pursued by designers and technician. In reality, this kind of interaction is highly affected by several factors, such as friction and, band loop options, loading positions, v-retainer arrangement and installation operation [4].

Mallet tapping is commonly recommended in industries as critical step during piping system assembly with clamp to alleviate the leaking problem of gas in the piping system which is possibly caused by the poor contact at certain area of the contact surface[5, 6]. Lightly mallet tapping the outer periphery of the clamp

to equalize the clamp tension is stipulated as standard installation procedure. However, the effect of mallet tapping on the contact pressure distribution and its working principle in solving sealing is still rare analyzed and the detailed location and operations of mallet tapping are still not normalized. One reason is that vibration caused by mallet tapping is analogous to the treatment of stress relief vibration applied on machine elements. Stress relief by vibration as an alternative method of heat treatment is widely used to release remaining stress, and uniform the distribution of residual stresses in industries [7].

Similarly, equalized contact pressure around the clamp can be acquired if stress relief by vibration also can occur to clamp and piping system after the correct excitation given by mallet tapping. Excitation force can cause high amplitude and low frequency vibration during a certain period of loading cycles. The resonant force combined with residual stresses could exceed the yield point and then caused plastic flow locally. As a result, the peak residual stresses are reduced and the stresses of structures are redistributed during the vibration [8]. Critical cyclic strain amplitude must be exceeded to relief stress and higher amplitude means more reduction in residual stress. Especially, resonant vibration is effective in almost complete relief surface stress of structures [9]. After stress distribution, static equilibrium can restore without alternation of tensioning strength or yield points. No further deformation will occur in the clamp, in another word, slack stiffness of clamp is increased and it becomes more resistant to small disturbance. Clamp band joint system's dynamic characteristic with respect to axial harmonic excitation is described theoretically and experimentally by Qin[10], but the effect of excitation on stress distribution of clamp is not emphasized.

In this paper, the mallet tapping effect on the contact pressure distribution of interference fit V-band clamp and piping systems is characterized since mallet tapping is deemed to provide a proper solution to marmon system leakage in industry. A piezoelectric sensor platform is set up to measure the contact pressure before and after mallet tapping at the initial stage of installation. The results support the mallet tapping procedure experimentally. Piezoelectric sensor is limited in initial stage of loading since the fragility of sensor material. The effect and mechanism of mallet tapping in the final assembly stage are concluded from dynamic behavior of clamp under external excitation. Transverse and longitudinal natural frequencies are derived using beam theory and verified by mallet tapping experiment test in order to estimate impulsive force response of clamp and piping system. Feasible suggestions for the clamp design and assembly will be introduced.

2. EXPERIMENT AND FEA RESULTS ABOUT CONTACT PRESSURE

In this research, piezoelectric sensor is chosen to measure the real radial clamping load distribution around V-band clamp. Compare with strain gauge usually attached to the periphery of clamp, the sensor should be place between V-band clamp and manifold, or between V-band clamp and bellow to approach the direct contact pressure distribution. In this case, piezoelectric polymer polyvinylidene fluoride (PVDE) is selected as sensor material in this research since ceramic and crystal materials are brittle and easy to break apart when installed between clamp and manifold with the pressure added on. While working with conventional readout electronics, imperfect insulating materials, and reduction in internal sensor resistance will result in a constant loss of electrons, and yield a decreasing signal. In fact, there are some applications that show quasi-static measurements. By selecting proper voltage follower (charge mode amplifier, Vout=Vin, Zin=∞, which has infinite impedance theoretically, while realistically the differential input impedance of the op-amp itself is from 1 MΩ to 1 TΩ), the output signal of piezoelectric sensor can be steady. The equivalent circuit and sensor platform with charge mode amplifier are Fig.1.

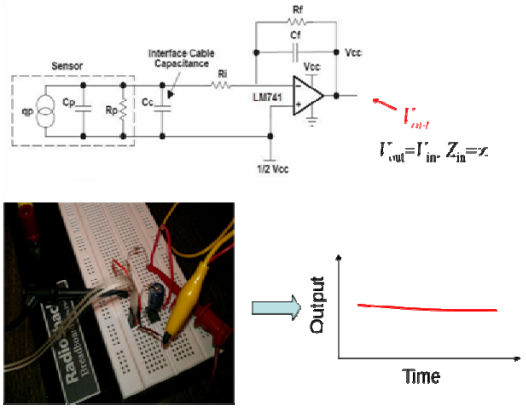

Figure 1. Piezoelectric PVDF sensor test platform

In order to get radial load data of V-band clamp from piezoelectric sensors, necessary calibrations are made before the experiment. With the calibration, the voltages of each sensor under different install torque on T-bolt are measured and then converted into pressure. The configuration of the clamp model used for the data measurement is shown in Fig.2, in which the T-bolt is not illustrated in the FEA model. A light load is applied to the holes of trunnion to simulate the toque applied on the T-bolt. FEA simulation is accomplished using half of the mode due to symmetry of this model. The model is meshed with 13345 elements, including tetrahedral, triangular, quadrilateral elements and so on. Constitutive behaviors are defined in the range of elastic because plastic deformation is not allowed in service. After getting the loading distribution of V-band clamp in the initial stage of loading from piezoelectric sensor test, special locations on clamp is tapped by plastic mallet to overcome static friction and redistribute radial load. The location of tapping points are at top left of back bend, top right of trunnion, and the gap between the V-shape retainer (Fig. 2).The capital letter stands for the location of sensor away from the top of the band.

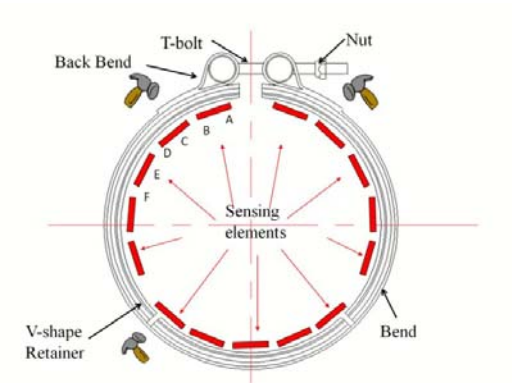

Figure 2. Configuration of clamp and tapping locations on clamp by softer mallet to equalize radial load

The contact pressures between bellow and V-retainers are illustrated in Fig.3. There are three pieces of V-retainers attached on the clamp band and the two upper pieces of V-retainers are of the same contact pressure distribution. Fig.3 (a) shows the upper piece of V-retainer pressure distribution and the distribution of the bottom V-retainer is shown in Fig. 3(b). The contact pressure before and after mallet tapping are differentiated using bold black and red lines. As to the bottom piece of clamp V-retainer, the center is the location presenting higher contact pressure since that location is the initial area contacting with the piping system. As to the upper piece of clamp V-retainer, the contact pressure increases from the bottom to the up overall except for three leaps which approximately fits well with the theoretical analysis given by Shoghi[2, 3]. Those contact pressure leaps can also be attributed as the remaining effect of the initial contact stress. Fig.3(c) shows the pressure distribution obtained from COMSOL multi-physics simulation with little load which aims to find the initial contact locations. Apart from that, the original model assembly is interference fit, thus the corresponding average contact pressures of the entire simulation are pretty low, but the results about the locations of those initial contact areas are apparent. The higher contact pressure distribution presented by simulation matched well with the piezoelectric sensor measurement, which proved the non-uniform distribution of pressure from the initial stage of installation.

The controlled measurement of contact pressure in Fig.3 verified the validity of mallet tapping during assembly. After mallet tapping, those locations with higher pressure experienced stress relief and the nearby lower compression locations experienced stress compensation accordingly. As a result, the gap between higher and lower pressure among different locations are reduced. It is important to point out that the pressure distribution at the bottom piece of V-retainer is decreasing from the center to two sides, which is inconsistent with the previous mentioned theoretical analysis [3]. That deviation confirmed the influence of initial contact and indicated the importance of equalize distribution from the beginning of installation procedure.

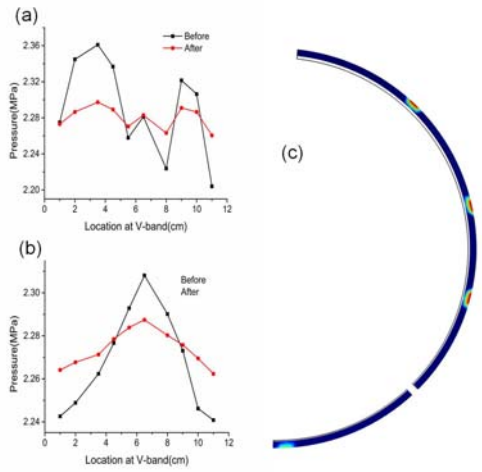

Figure 3. Contact pressure under Torque 5Nm (a) Before mallet tapping (b) After mallet tapping on special locations of V-band clamp, (c) COMSOL simulations. The location in (a) is the distance away from the upper of the band.

3. MECHANISUM ANALYSIS OF MALLET TAPPING

The controlled experiment and FEA simulation results in the initial stage of installment are reliable when the T-bolt is still straight and clamp are in perfect round. However, in reality, T-bolt bends downward and ovalization of clamp occurs at the nearby of loading zone. Those consequences are unavoidable considering current design of clamp and installment procedure. Especially, the warping effect due to the ovalization of clamp causes the low stress in the zone beneath the back bend which is close to the peak stress area. To reach an equalized tension around the clamp band, the mallet tapping and tightening of torque should be repeated until the service torque is reached or further movement is invisible. As an effective optimization method, the mallet tapping is utilized continually with the increasing of torque during entire installment procedure.

There are many reasons to account for the optimization effect of mallet tapping. First, the circumferential component of the tapping enforces the circumference movement of clamp to remit the warping of clamp after ovalization, and the radial component of the tapping keeps the clamp in good contact with the piping systems and holds the new equilibrium of stress distribution. At the same time, further torque is applied to maintain the mallet tapping effect. Second, contact pressures from bottom to top of clamp are in exponential increase if the warping effects are remitted totally according to the theoretical analysis. However, this distribution is not reliable without the existence of friction. Thus, transient separation between clamp and piping system in a certain part of contact area can promote pressure redistribution. The superposition of stress redistribution after mallet tapping leads to equalization of contact pressure on the entire clamp.

The third reason is vibration effect analogous to the VSR principle where the vibration caused by the mallet tapping breaks the force equilibrium at the high stress

locations. The peak stresses beneath trunnions are relaxed after the reconstruction of the new equilibrium. There are several types of errors in manufacturing, setting error due to the misalignment of T-bolts and nut during assembly, positioning error caused by clamp deflection, and machining tolerance. As to clamp assembly, different operation procedures lead to setting errors which causes abnormal stress distribution. One of the most significant benefits of VSR is that it can relieve the peak stresses at any points in many types of manufacturing and installation process. High amplitude and low frequency vibration in a certain period of time can be introduced by period exciting force, which will be the most effective and fastest way to relieve residual concentrated stresses because of the possible "resonant force".

From the effectiveness of VSR, dynamic response of clamp upon impulsive force is motivated to account for the vibration effect of mallet tapping and detailed discussed is presented in the following. The input of mallet tapping force is treated as impulsive force and its response upon with the transverse and longitudinal impulse are discussed separately. To predict the mode of vibration wave upon Impulsive force, natural frequencies of the clamp and the piping system is estimated theoretically and experimentally.

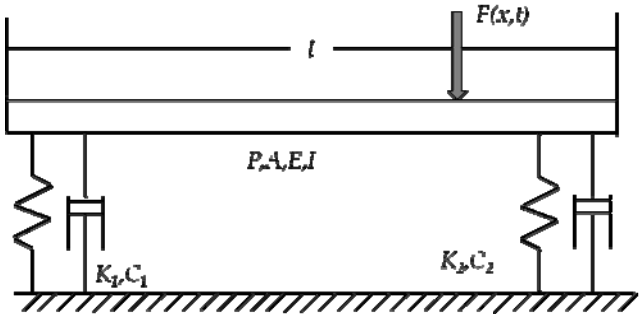

Figure 4. Transverse vibration of beam under forced load

3.1 **Theoretical estimation**

Natural frequencies in transverse and longitudinal are derived by a beam-spring-damping system. The model shown in Fig. 4 is applied to acquire the wave equation of clamp without initial load and moment in the transverse direction. Assuming uniform properties of clamp, the wave equation is given as,

$$-C^{*2}\frac{\partial^4 y}{\partial x^4}=\frac{\partial^2 y}{\partial t^2} \tag{1}$$

Where $C^*=\sqrt{EI/\rho}$, EI is the stiffness of beam, E is 200×10^9, the average inertia I is 1.57×10^{-9}Nm^4 and density ρ is 7850kg/m^3. Rewrite y as $y(x,t)=Y(x)G(t)$ to obtain two solutions for *Y(x)* and *G(t)* seperately as, $Y(x)=A_3\sinh(\beta x)+A_4\cosh(\beta x)+A_5\sin(\beta x)+A_6\cos(\beta x)$ and $G(t)=A_1\sin(\omega t)+A_2(\cos\omega t)$. A_3, A_4, A_5, and A_6 are coefficients to be determined with boundary conditions, β is $\sqrt{\omega/C^*}$ and *ω* is frequency. Substitute *Y(x)* into the boundary conditions described in the following Equations from (2) through (7),

Moment, $M=EI\dfrac{d^2Y(0)}{dx^2}=0$ (2a)

From Equation (4a), it can be derived that

$A_6=A_4$ (2b)

Force, $F=EI\dfrac{d^3Y(0)}{dx^3}=-K_1[Y(0)]-C_1(Y(0))'$ (3a)

which yields

$$A_3(EI\beta^3+C_1\beta)+A_4*2K_1+A_5(-EI\beta^3+C_1\beta)=0 \tag{3b}$$

Moment, $M=EI\dfrac{d^2Y(l)}{dx^2}=0$; (4a)

From Equation (6a), we obtain

$$\begin{aligned}&A_3\sinh(\beta l)+\\&A_4(\cosh(\beta l)-\cos(\beta l))+A_5(-\sin(\beta l))=0\end{aligned} \tag{4b}$$

Force, $F=EI\dfrac{d^3Y(l)}{dx^3}=-K_2[Y(l)]-C_2(Y(l))'$ (5a)

From which the following equation is derived:

$$\begin{aligned}&A_3(EI\beta^2\sinh(\beta l)+K_2\sinh(\beta l)+C_2\beta\cosh(\beta l))+\\&A_4\{EI(\beta^3\sinh(\beta l)+\beta^3\sin(\beta l))+K_2(\cosh(\beta l)+\\&\cos(\beta l))+(\beta\sinh(\beta l)-\beta\sin(\beta l))C_2\}+\\&A_5(-EI\beta^3\cos(\beta l)+K_2\sin(\beta l)+C_2\beta\cos(\beta l))=0\end{aligned} \tag{5b}$$

K_1, K_2, C_1, and C_2 are spring stiffness and damping coefficients, which are estimated with clamp's properties. In order to get non-trivial solutions A_3, A_4, A_5, and A_6 to satisfy the Equations (2b), (3b), (4b) and (5b) together, the solution of of β should be 6.45 and the correspondng natural frequency ω is 9.04. With the non-trival solutions of coefficients A_3, A_4, A_5 and A_6, the natural vibration of clamp can be rewritten as,

$$y(x,t)=\sum_{i=1}^{\infty}Y_i(x)b_i\sin(\omega_i t+\phi_i) \tag{6}$$

b_i and φ_i can be derived from initial boundary conditions. On the basis of transverse natural frequency of beam without forced load, the response of transverse impulsive force is analyzed. First of all, the impulsive force applied on the back bend of clamp is defined using Dirac distribution *δ(t)*,

$$p(x,t) = P\delta(t-\tau)\delta(x-\xi), \quad (7)$$

where *P* is force, *τ* is time and *ζ* is the location of mallet tapping. Wave equation of transverse vibration with forced impulse can be written as,

$$EI\frac{\partial^4 y}{\partial x^4} + \rho A\frac{\partial^2 y}{\partial t^2} = p(x,t) - \frac{\partial m(x,t)}{x} \quad (8)$$

Moment m*(x,t)* is 0 in current case. To get the general solution of this equation, call for the orthogonality about mass and stiffness,

$$\int_0^l \rho A Y_j Y_i dx = 0 \quad (9a)$$

$$\int_0^l Y_j (EIY_i'')''dx = 0 \quad (9b)$$

$Y_i(x)$ and $Y_j(x)$ are corresponding to frequencies ω_i and ω_j, where Y_j is the j^{th} order of mode.
Normalized $Y_i(x)$ to get canonical mode as shown in Equation (10),

$$Y_j^{'}(x) = 0.212Y_j(x) \quad (10)$$

Forced impulse vibration written with canonical mode is presented as,

$$y(x,t) = \sum_1^\infty Y_i(x)\eta(t), \quad (11)$$

$\eta_i(t)$ is canonical coordinates. Substitute it into governing equation and define the initial boundary condition as,

$$y(x,0) = f_1(x) = \sum_1^\infty Y_i(x)\eta_i(0), \quad (12a)$$

$$\frac{\partial y}{\partial t}|_{t=0} = f_2(x) = \sum_1^\infty Y_i(x)\eta_i(0)' \quad (12b)$$

The general solution of the i_{th} canonical coordinate is

$$\eta_j(t) = \eta_i(0)\cos(\omega_j t) + \frac{\eta'_j(0)\sin\omega_j t}{\omega_j} + \frac{1}{\omega_j}\int_0^t q_j(\tau)\sin\omega_j(t-\tau)d\tau \quad (13)$$

For zero initial conditions, clamp's response to transverse forced impulse can be represented as,

$$y(x,t) = \sum_1^\infty \frac{1}{\omega_j} Y_j(x)Y_j(\zeta)P\sin(\omega_j(1.6-0.078)) \quad (14)$$

Where 1.6 is total time of response, 0.078 is the mallet tapping time, *P* is 200mN, and the integration length used to derive Equation (14) is 0.484m. All those data are determined from mallet tapping experiment.
Similarly, response of clamp after longitudinal impulsive force is analyzed. Hamilton's principle is utilized to obtain the wave equation in longitudinal direction. The kinetic energy function for the elastic clamp is,

$$T = \frac{1}{2}\int_0^L \rho A(\frac{\partial u}{\partial t})^2 dx, \quad (15)$$

The potential energy function is,

$$V = \frac{1}{2}\int_0^L EA(\frac{\partial u}{\partial x})^2 dx + \frac{1}{2}k_1[\frac{\partial u}{\partial x}(0,t)]^2 + \frac{1}{2}k_2[\frac{\partial u}{\partial x}(L,t)]^2, \quad (16)$$

Define the Non-conservative forces damping as virtual work δW_{nc}. The extended Hamilton's Principle is written as,

$$\int_{t1}^{t2}(\delta T - \delta V + \delta W_{nc})dt, \quad (17)$$

The order of variation and integration are interchangeable. Part of variations are considered separately from Equation (18) to (20)

$$\delta W_{nc} = -C_1\frac{\partial u}{\partial t}(L,t)\delta u(L,t) - C_2\frac{\partial u}{\partial t}(0,t)\delta u(0,t) \quad (18)$$

$$\frac{1}{2}\int_{t1}^{t2} k\delta[u(L,t)]^2 dt = \int_{t1}^{t2} ku(L,t)\delta u(L,t)dt \quad (19)$$

$$\frac{1}{2}\int_{t1}^{t2}\delta\int_0^L \rho A(\frac{\partial u}{\partial t})^2 dxdt = -\int_{t1}^{t2}\int_0^L \rho A\frac{\partial^2 u}{\partial t^2}\delta u dxdt \quad (20)$$

Combine variation items and substitute into Hamilton's principle. Integration leads to,

$$EA\frac{\partial^2 u}{\partial x^2} = \rho A\frac{\partial^2 u}{\partial t^2}, \quad (21)$$

Boundary condition is set according to principle of virtual work,

$$EA\frac{\partial u}{\partial x}(0,t) - ku(0,t) - c\frac{\partial u}{\partial t}(0,t) = 0, \quad (22)$$

$$-EA\frac{\partial u}{\partial x}(L,t) - ku(L,t) - c\frac{\partial u}{\partial t}(L,t) = 0, \quad (23)$$

Similarly, k and c are spring stiffness and damping coefficient. Procedures to solve natural frequency are similar to transverse vibration equations. The general solution about longitudinal wave equation can be written as, $u(x,t) = G(t)F(x)$ or

$$u(x,t) = (B_1 \sin(\omega t) + B_2 \cos(\omega t))(B_3 \sin(\frac{\omega}{c^*} x) + B_4 \cos(\frac{\omega}{c^*} x))$$

Damping coefficient has very limited effect on ω/c*, where c* is $(E/\rho)^{1/2}$. Substitute the general solution *F(x)* into the following boundary conditions,

$$EAB_3 \frac{\omega}{c} - kB_4 = 0 \quad (24a)$$

$$-EA\left\{B_3 \frac{\omega}{c^*} \cos(\frac{\omega}{c^*} L) - B_4 \frac{\omega}{c^*} \sin(\frac{\omega}{c^*} L)\right\} - k\{B_3 \sin(\frac{\omega}{c^*} L) + B_4 \cos(\frac{\omega}{c^*} L)\} = 0 \quad (24b)$$

Similarly, to guarantee nontrivial solutions, the ω/c* is equal to 6.49 and natural frequency is 3.27×10^4 rad/sec. Then, the non-trival solutions of coefficience B_3 is close to 0 and B_4 is close to 1. Finally, the general mode of vibration wave after longitudinal impulsive force can be presented as,

$$u(x,t) = \cos(6.5x)(B_1 \sin(\omega t) + B_2 \cos(\omega t)) \quad (25)$$

Again, do normalization to get principle vibration mode,

$$u_j'(x) = D_j u_j(x) \quad (26)$$

D_1 is 2.247 for the first vibration wave mode. Those parameters used to calculate mode of vibration wave after mallet tapping are the same as those parameters used in transverse response calculation. Apply the similar orthogonality coordination and obtain orthogonality mode, the longitudinal vibration wave with impulsive force can be represented as,

$$u(x,t) = \sum_1^{\infty} \frac{1}{\omega_i} U_i(\xi) U_i(x) P \sin \omega_i (1.6 - 0.078) \quad (27)$$

3.2 **Experiment verification**

Mallet tapping experiment is carried out to complement the theoretical estimation of frequencies in longitudinal and transverse directions. Laser sensor and acceleration sensor are set up to collect the response after mallet tapping and the time domains are shown in Fig. 5(a) and (b). N is the number of collected data.

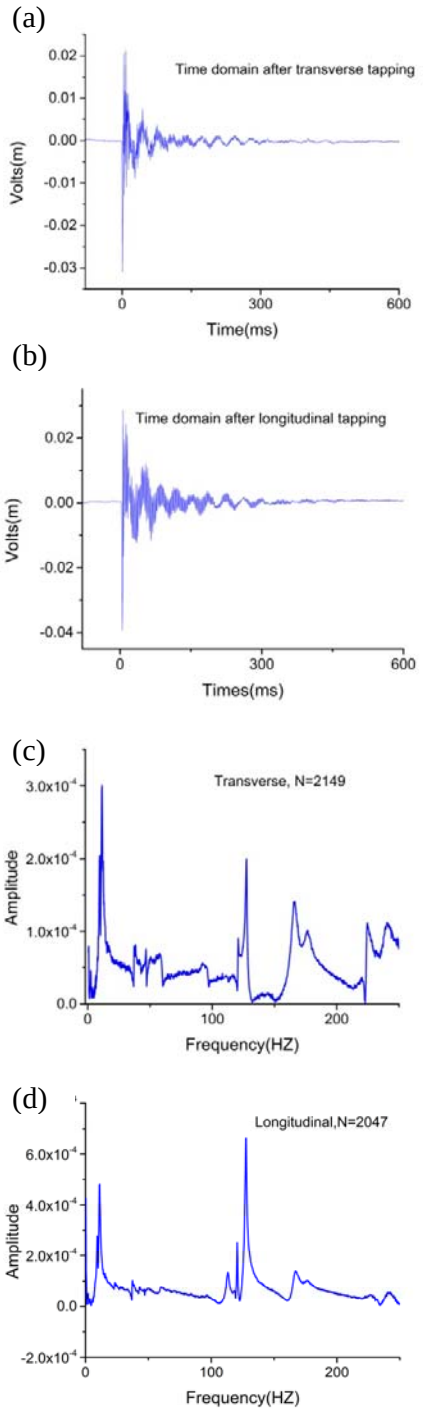

Figure 5. Time domains after mallet tapping (a) Transverse tapping, (b) Longitudinal tapping; Frequency domains (c) Transverse tapping, ωd =11.12; (b) Longitudinal tapping, ωd =127.69.

Frequency domains are analyzed by Fast Fourier Transform (FFT) and the results are represented in Fig.5 (c) and (d). From the frequency analysis, the damped frequency ω_d in transverse and longitudinal direction are 11.12 and 127.69 respectively. Damping factors ξ obtained from time domain are 0.085 and 0.026, respectively for transverse and longitudinal impulsive force. The mass of clamp is 0.156kg and

marmon is 8.53kg. The corresponding natural frequency can be determined from a relationship, $\omega_n = \omega_d \Big/ \sqrt{1-\xi^2}$.

The calculated natural frequency ωn is 11.15 in transverse and 127.73 in longitudinal direction. The natural frequency calculated based on experiment test is pretty close to theoretical estimation in transverse but apparently different in longitudinal direction. The frequency difference in longitudinal direction can be attributed to model selections applied in experiment and theoretical analysis. In theoretical analysis, clamp is treated as independent model, while the clamp is combined with the piping systems as one model in the vibration experiment test. Just like in bending deflection analysis of clamp, moment of inertia should include the entire piping systems rather than merely clamp. If not that, the estimated radial deflection could be as large as half radius of clamp, which is not practical. Hence, frequency in the longitudinal direction from the experiment test is much lower than theoretical analysis and the theoretical calculation presents a better approximation.

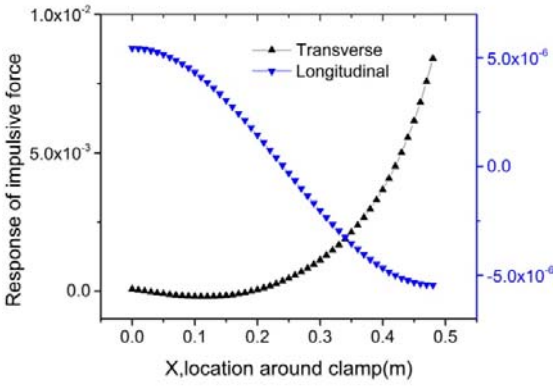

Figure 6. The first mode of vibration wave after impulsive force applied on clamp.

With the estimated frequencies from theoretical calculation and experiment tests, the first modes of vibration waves after mallet tapping are present in Fig.6. The upper triangle line stands for response upon transverse impulsive force which is higher than the response upon longitudinal force by almost four orders of magnitudes. Thus, transverse components of mallet tapping plays the dominate role in contact pressure redistribution. Variation of mallet tapping locations merely affects the amplitude of vibration wave as shown in Equation (14) and (27). Considering the feasibility of mallet tapping among various mechanical parts, back bend is selected as tapping location in Fig 10. The displacement of the band is negative from 0.03 to 0.2m, and turns to positive in the range of 0.2 to 0.5m. Due to the boundary condition of manifold flange, the negative displacement of the band is forced to zero, and it makes the positive displacement from 0.2 to 0.5m even slightly larger. From 0 to 0.2m, the displacement of the band is almost a constant, but, it ramped quickly after the displacement turns to positive. Therefore, if the mallet impulse is applied next to the end of the left back bend, the friction force under the right half band will be evenly released, and the contact pressure distribution on the right side will follow the pattern of exponentially decrease from top to bottom. If another mallet impulse is applied to the symmetric location on the right side, the similar effect will occur on the left half band. Since the negative displacement is forced to zero by the manifold flange, the contact pressure distribution will not be disturbed. At the end of these two mallet impulses, the optimized contact pressure distribution under the whole V-retainer will be achieved. At this time, applying a small tightening torque onto the nut can keep the newly achieved optimal contact pressure distribution unchanged.

4. CONCLUSION

In this paper, a sensor platform with charge mode amplifier was set up to measure the contact pressure between V-retainer and piping systems. The results indicated non-uniform contact pressure and verified with the complement of FEA simulation. Initial contact area generated higher pressure from the very beginning of installment and dwelled on the remaining distribution under higher load. Mallet tapping was applied to equalize the pressure distribution and the controlled test results proven its validity during installment. Possible reasons about the principle of mallet tapping were discussed. Besides of those, theoretical and experiment models were built to have more depth exploration. The first mode of vibration wave after mallet tapping on clamp back bend were calculated and that results reasonably explained the working principle of applying mallet tapping during the entire clamp installment procedure.

5. REFERENCES

[1] Marman clamp system design guidelines, Guideline GD-ED-2214, NASA Goddard Space F light Centre, 2000.
[2] K. Shoghi, S. Barrans, and H. Rao.(2004), "Stress in V-section band clamps," *Proceedings of the Institution of Mechanical Engineers, Part C: Journal of Mechanical Engineering Science,* vol. 218, pp. 251-261.
[3] K. Shoghi, H. Rao, and S. Barrans.(2003), "Stress in a flat section band clamp," *Proceedings of the Institution of Mechanical Engineers, Part C: Journal of Mechanical Engineering Science,* vol. 217, pp. 821-830.
[4] G. L. Jones.(1980), "Evaluation of clamp effects on LMFBR piping systems," Swanson Engineering Associates Corp., McMurray, PA (USA).
[5] D. C. Bahler.(1990), "V-clamp installation tool," ed: Google Patents.
[6] D. C. Bahler.(1988), "Method of using V-clamp installation tool," ed: Google Patents.
[7] G.-C. Luh and R. Hwang.(1998), "Evaluating the effectiveness of vibratory stress relief by a modified hole-drilling method," *The International Journal of Advanced Manufacturing Technology,* vol. 14, pp. 815-823.
[8] R. McGoldrick and H. E. Saunders,(1943), "Some experiments in stress relieving castings and welded structures by vibration," *Journal of the American Society for Naval Engineers,* vol. 55, pp. 589-609.
[9] D. Moffat.(1980), "Vibratory stress relief: a fundamental study of its effectiveness," *Materials and Technology*.
[10] Z. Qin, S. Yan, and F. Chu.(2010), "Dynamic analysis of clamp band joint system subjected to axial vibration," *Journal of sound and vibration,* vol. 329, pp. 4486-4500.

Mechanism and Effect of Mallet Tapping on Contact Stress Distribution Between V-band Clamp and Piping Systems

Zhengui Zhang, Haiyan H Zhang, Peixuan Wu

Primljen (02.02.2014.); Recenziran (27.05.2014.); Prihvaćen (30.06.2014.)

Rezime

Ovaj rad je posvećen istraživanju mehanizma poznatog kao 'mallet tapping' na izjednačavanje raspodele kontaktnog pritiska između V-pojasne stege i cevovodnog sistema. Senzorska platforma sa pojačavačem promene naboja je ugrađena kako bi sakupljala kvazi-statična merenja kontaktnog pritiska tokom opterećenja. Kontaktna opterećenja u početnoj fazi pre i posle 'mallet tapping' procesa se mere pomoću testova piezoelektričnih senzora. Analiza konačnih elemenata je izvršena kako bi se pronašla početna kontaktna područja. Kontrolisano merenje verifikovalo je održivost ovog procesa na redistribuciju kontaktnog pritiska. Što se tiče stabilnosti stege, efekat ovog procesa se diskutuje sa spektra radnog principa VSR. Dinamička analiza je takođe pokušana kako bi se istražio mehanizam 'mallet tapping' na ujednačavanje raspodele kontaktnog pritiska. Frekvencije stege su procenjene teoretskom kalkulacijom i eksperimentalnim testovima, koji su primenjeni kako bi se razvio princip vibracionog talasa nakon primene 'mallet tapping'.

Ključne reči: *kontaktni pritisak, 'Mallet tapping', V-pojasna stega, VSR*